16th World Conference on Earthquake, 16WCEE 2017

Santiago Chile, January 9th to 13th 2017

Paper N° 1055 (Abstract ID)

Registration Code: S-T1461976109

TIME-DEPENDENT SEISMIC HAZARD ABOVE THE SOUTH AMERICA SUBDUCTION ZONE IN CENTRAL AND SOUTHERN CHILE

I. Wong[(1)], M. Dober[(2)], P. Thomas[(3)], E. Nemser[(4)], J. Bott[(5)]

[(1)] *Principal Seismologist, Lettis Consultants International, Inc., wong@lettisci.com*
[(2)] *Project Seismologist, AECOM, mark.dober@aecom.com*
[(3)] *Senior Earthquake Engineer, Lettis Consultants International, Inc., thomas@lettisci.com*
[(4)] *Senior Seismic Geologist, AECOM, eliza.nemser@aecom.com*
[(5)] *Senior Seismologist, AECOM, jacqueline.bott@aecom.com*

Abstract

The Peru-Chile portion of the South America subduction zone is one of the most seismically active regions in the world and the source of some of the largest known earthquakes, including the 1960 moment magnitude (**M**) 9.5 Great Chile earthquake and more recently, the 2010 **M** 8.8 Maule earthquake. Since the beginning of the historical record in the mid-1500s, there have been at least 10 earthquakes of **M** 8 and larger principally due to rupture of the megathrust based on reported tsunamis. We have performed probabilistic seismic hazard analyses (PSHA) for four cities above the subduction zone in central and southern Chile. We have included a time-dependent model for the region's most significant seismic source, the two southernmost segments of the South America subduction zone megathrust: the Concepcion-Valparaiso and Southern Chile segments. Our time-dependent model is based principally on the historical record and the challenge was to characterize the significant uncertainties in the segmentation, recurrence, and maximum magnitudes of the megathrust earthquakes that have occurred and will occur along the subduction zone. The PSHA seismic source model also includes crustal faults, crustal background seismicity, and the Wadati-Benioff zone. A number of crustal faults are located above the South America megathrust although it is unclear whether these are independent seismic sources or rupture coseismically with the megathrust.

An additional critical issue that needs to be addressed in the PSHA is the selection of ground motion prediction models. We used the Next Generation of Attenuation (NGA)-West2 models for the crustal seismic sources and recent global models for both the megathrust and the Wadati-Benioff zone. We also compared these latter models with the strong motion data from the 2010 Maule earthquake.

Assuming generic soil site conditions, we computed the hazard for the cities of Valparaiso, Concepcion, Temuco, and Puerto Montt. We compare our probabilistic hazard results with a time-independent model of the two southern segments of the South America megathrust to evaluate the impact of the time-dependent model on the hazard in central and southern Chile.

Keywords: probabilistic seismic hazard analysis; South America subduction zone; Chile

1. Introduction

We have performed site-specific seismic time-dependent and time-independent hazard analyses of four cities in central and southern Chile (Valparaiso, Concepcion, Temuco, and Puerto Montt), above the Peru-Chile portion of the South America subduction zone, one of the most seismically active regions in the world (Figs. 1 and 2). The region was the site of the largest known earthquake, the 1960 moment magnitude (**M**) 9.5 event and it is expected that the earthquake will be repeated in the future. More recent earthquakes have also shaken Chile including the 27 February 2010 **M** 8.8 Maule earthquake (Figs. 1 and 2).

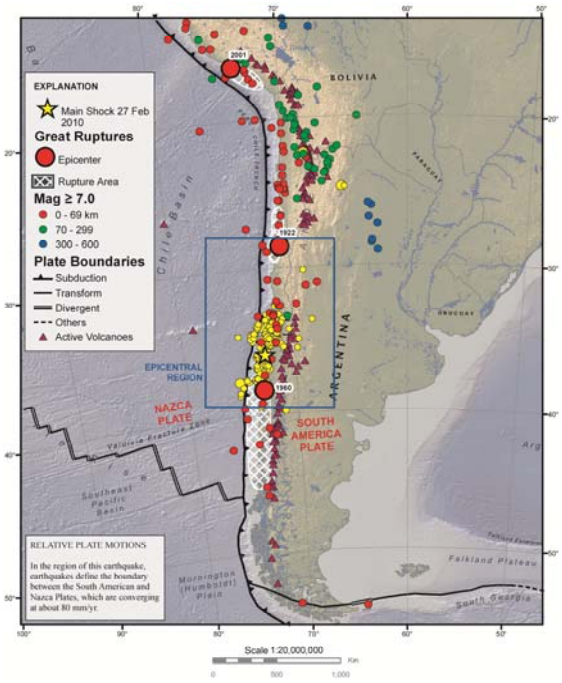

Fig. 1 – Tectonic setting of Chile (Source: USGS).

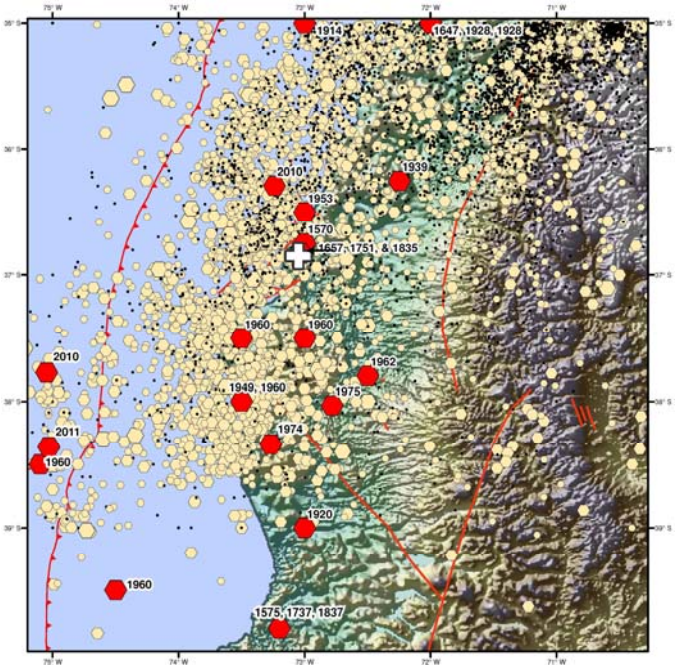

Fig. 2 – Historical seismicity of site region 1562-2012. (**M** ≥ 3)

The primary objective of this study was to estimate the future levels of ground shaking at these cities that will be exceeded at specified probabilities by performing time-dependent and time-independent probabilistic seismic hazard analyses (PSHA). Available geologic and seismologic data were used to evaluate and characterize potential seismic sources, the likelihood of earthquakes of various magnitudes occurring on those sources, and the likelihood of the earthquakes producing ground motions over a specified level. It should be noted that there are significant uncertainties in the characterization of seismic sources and ground motions in Chile due to the limited research in active faulting and to a lesser extent, strong motion seismology; these uncertainties have been incorporated into the PSHA.

2. PSHA Methodology

The PSHA approach used in this study is based on the model developed principally by Cornell [1]. The occurrence of earthquakes on a fault is assumed to be a Poisson process. The Poisson model is widely used and is a reasonable assumption in regions where data are sufficient to provide only an estimate of average recurrence rate [1]. The occurrence of ground motions at a site in excess of a specified level is also a Poisson process, if (1) the occurrence of earthquakes is a Poisson process, and (2) the probability that any one event will result in ground motions at the site in excess of a specified level is independent of the occurrence of other events. The calculations were made using the computer program HAZ38 developed by N. Abrahamson. This program has been validated in the Pacific Earthquake Engineering Research (PEER) Center-sponsored "Validation of PSHA Computer Programs" Project [2].

3. Seismotectonic setting

The South Ameica plate overrides the subducting oceanic Nazca plate; deformation in Chile is driven by this active subduction zone and related tectonic processes. The Peru-Chile portion of the South America subduction zone has been the source of some of the largest earthquakes in the world. In addition to great megathrust earthquakes along the interface between the South America and Nazca plates, there has been abundant seismicity

in the crust of the South America plate (above a depth of about 40 to 50 km) and intraslab seismicity within the Nazca plate.

The Liquiñe-Ofqui fault zone (LOFZ) is a major margin-parallel transpressional dextral fault system that accommodates a significant portion of the strike-slip motion along this oblique subduction zone in south-central Chile (e.g., [3]) (Fig. 3). In the kinematic framework of the plate boundary system, the LOFZ forms the eastern boundary of the Chiloé microplate, a forearc sliver that is effectively decoupled from the stable South America Plate [3, 4]. The LOFZ has been active as a transpressional dextral structure since the Pliocene, with a long-term (6 Ma) slip rate of 13 ± 3 mm/yr in the northern domain (38°S – 42°S) [3]. However, based on geodetic data and finite-element modeling, Wang *et al*. [4] show that over the past ~6 Ma, the strike-slip rate of the LOFZ has decreased to a present value of 6.5 mm/yr in the northern domain, with the slip rate decreasing northwards to zero at the intersection with the Lanalhue fault (LF).

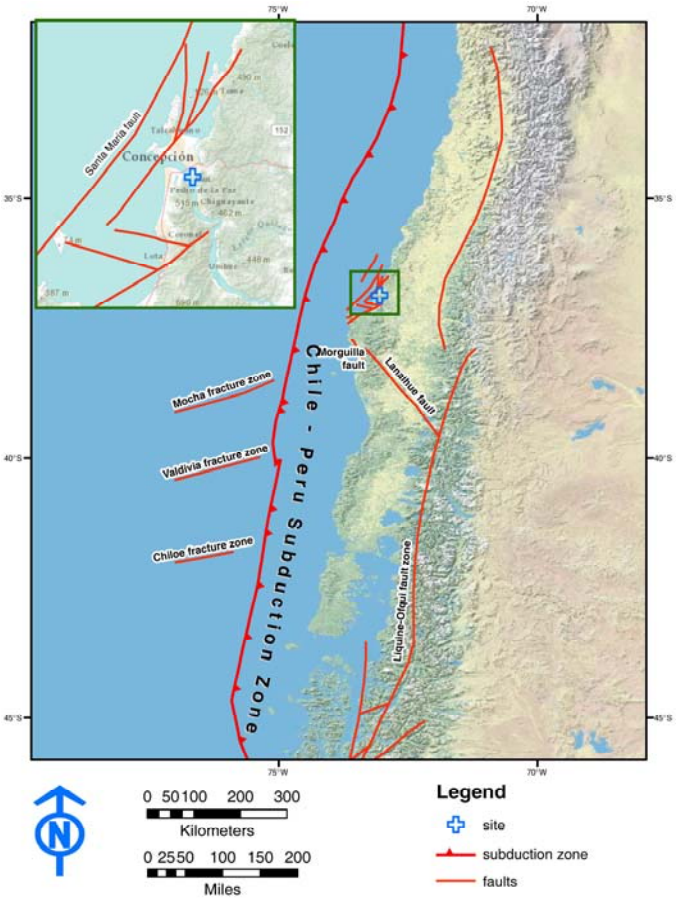

Fig. 3 – Crustal faults included in PSHA.

GPS data suggests that the Chiloé microplate is rotating and translating northward against a buttress formed by the Arauco-Nahuelbuta block. Rotation of the Chiloé forearc sliver is accommodated by deformation (including shortening and right-lateral slip) across the LF that forms the northern boundary of the microplate [5] (Fig. 3). Seismic reflection data, focal mechanisms, and hypocenter distributions indicate that the LF is a steep, NE-dipping fault. Quaternary activity along the LF is evident as it cuts fluvial and alluvial terraces of the Plio-Quaternary Malleco Formation [6].

Slip models for the 2010 **M** 8.8 Maule megathrust earthquake indicate that the Santa María fault system (SMFS) is located within a region of reduced slip between two high-slip patches [7] (Fig. 3). Melnick *et al*. [8] interpret this correspondence to suggest that strain release along the SMFS may impact the rupture behavior of the megathrust. There is evidence that other forearc structures may affect slip on the megathrust: Melnick *et al*.

[6] note that the large-magnitude events from the 1960 **M** 9.5 megathrust earthquake sequence (which included four foreshocks up to **M** 8.2 and a major **M** 7.9 aftershock) occurred about 35 to 50 km depth along a NW–SE region that is spatially coincident with the Lanalhue fault [6].

4. Historical seismicity

An historical earthquake catalog was compiled for the site region as shown in Fig. 2. Primary data sources include catalogs from the U.S. Geological Survey's (USGS) National Earthquake Information Center Preliminary Determination of Epicenters for 1973 through 2012, Centro Regional de Sismologia para America del Sur (CERESIS) for 1562 through 1981 (SISRA), el Servicio Sismologico de la Universidad de Chile (GUC) for 1570 through 2012 (instrumental epicenters only since 2000), the International Seismological Center (ISC) for 1914 through 2009, and the National Oceanic and Atmospheric Administration's National Geophysical Data Center database of significant earthquakes (1562-1985). All known events are included in the catalog and thus a minimum magnitude threshold was not maintained throughout. The catalog contains nearly 7,000 earthquakes from October 1562 through mid-January 2012. Over half of the earthquakes listed in the earthquake catalog are aftershocks of the 2010 Maule earthquake.

Since 1562, a total of 25 earthquakes larger than approximately **M** 7 have been recorded or reported and are thought to have occurred in the study region (Fig.2). A total of 14 events occurred prior to adequate seismographic coverage and so there is a paucity of information on these events; their locations and magnitude estimates can be highly uncertain. At least eight very large earthquakes are thought to have occurred along the megathrust and produced damaging tsunamis in 1570, 1575, 1657, 1751, 1835, 1928, 1960 and 2010 (Fig.2). Some of these events ruptured to the north or to the south from outside of the study region. One very large intraslab earthquake (surface wave magnitude [M_S] 7.9) occurred close to Chillán in 1939 at a depth of between 80 and 100 km.

Haberland *et al*. [9] performed an earthquake location and velocity model inversion for the forearc region south of Concepcion, near the northern nucleation point of the 1960 earthquake (between 37ºS and 39ºS). About 214 earthquakes were recorded on a dense temporary seismic array (November 2004 to June 2005) which included ocean bottom seismometers. Crustal earthquakes were located at depths between 10 and 30 km, cutting right through the forearc crust, some of which were located along the LF which appears to be a vertical fault at depth based on the hypocenter locations. In this study, because the earthquake locations are not as accurate as those obtained using a dense seismic array, we have selected crustal earthquakes to be those occurring at less than 50 km depth. Earthquakes east of the base of the subduction zone and less than 50 km depth were assigned as crustal events. Earthquakes that occurred below depths of 50 km and east of the subduction zone interface were assigned as intraslab events.

Many of the larger events within the study region are occurring on the downgoing slab at depths down to 200 km. The activity of the slab is diffuse and distributed throughout the subducting Nazca plate. Based on well-located seismicity [9], the subducting plate appears to dip at a shallow angle of around 25º eastward. Based on the Maule earthquake, the megathrust itself dips about 12º to the east. Examination of the historical seismicity shows only a moderate level of crustal seismicity in the study region.

5. Seismic source characterization

Active and potentially active seismogenic crustal faults, the South America subduction zone (both megathrust and intraslab zones), and background crustal seismicity are the seismic sources significant to the study region in terms of strong ground shaking. Potentially significant active crustal faults were identified and assessed solely through a review of existing literature and data. It is important to emphasize that the inventory of active crustal faults in central-south Chile should be considered incomplete. Several recent active fault investigations have been performed in the region, though no paleoseismic investigations have been conducted to decipher prehistoric earthquake rupture behavior along the active faults. The collaborative compilation published by the USGS *Maps and Database of Quaternary Faults in Bolivia and Chile* [10] does not include active faults in the study region,

and therefore our characterization is primarily based on published fault studies in the study region that have been published in the past 5 years.

5.1 Crustal fault sources

In our analysis, we included all known Quaternary faults within the study region (Fig.3). These crustal fault sources were judged to be active because they display evidence for Quaternary movement (i.e., displacement in the past 1.6 million years). Little is known about the earthquake rupture behavior of crustal Quaternary faults in central and southern Chile so our rupture models are relatively simple. Because the crustal faults included in this analysis are forearc structures that rupture coseismically with the megathrust but have also been shown to rupture independently, we have included both independent and dependent (linked) alternatives in our analysis. For the SMFS, we favor the latter (weighted 0.7) based on evidence that the fault system ruptured during the 1751, 1835, and 2010 megathrust events [6, 8]. In the absence of specific data on the earthquake history of the other faults included in this analysis, we adopt the same weighting scheme.

For all rupture models (independent and linked), faults are modeled as planar sources that extend the full depth of the seismogenic crust. Thus, fault dips for all of these rupture models are averages estimated over the full depth of the seismogenic crust. The thickness of the seismogenic crust was estimated at 30 ± 2 km for the LF and 27 ± 2 km for all other crustal fault sources based on observed seismicity and slab geometry [9]; values represent the average depths at which the faults root into the plate interface.

Maximum magnitudes for thrust faults were estimated using the empirical relationships based on fault rupture length and rupture area of Wells and Coppersmith [11] for all types of faults. Resulting expected magnitudes from the two relations were calculated using preferred geometrical parameters and averaged to determine the preferred magnitude (weighted 0.6). Hanks and Bakun [12] demonstrated that for strike-slip faults, the data for historical earthquake ruptures better fit a bilinear regression based on rupture area. Therefore, for the LF we use their relations based on rupture area, and the Wells and Coppersmith [11] relation based on surface rupture length (averaged with equal weight) to determine preferred maximum magnitudes (weighted 0.6). To account for the various uncertainties in estimating maximum magnitudes, we also included ± 0.3 magnitudes (weighted 0.2 each) for all of our maximum magnitude distributions.

The characteristic, maximum magnitude, and truncated exponential recurrence models were used for the crustal faults in the PSHA and weighted 0.6, 0.3, and 0.1, respectively. The timing of earthquakes on active crustal faults in the region is unknown and so recurrence intervals for earthquake ruptures on faults are also unknown. Therefore, we used slip rates (in mm/yr) to characterize the rate of earthquake activity for crustal fault sources. Though there have been several recent efforts to constrain slip rates along the crustal sources included in this analysis, the broad distribution of slip rates included in our characterization reflects the substantial uncertainty in these estimates.

5.2 Crustal background seismicity

Crustal background or random earthquakes are those events that can occur without an apparent association with a known or identified tectonic feature. Within the Andean crust of the site region, seismicity is distributed diffusely with no clear relationships with any geologic structures. These faults are often called “blind” or “buried” faults. The hazard from such sources is incorporated into the PSHA through inclusion of an areal source zone and Gaussian smoothing weighted equally.

Crustal background earthquakes are assumed to occur throughout the study region. We estimate the maximum magnitude for the background earthquakes to be between **M** 7.0 and 7.5, weighted 0.7 and 0.3, respectively. Earthquakes larger than **M** 6.5 to 7.0 will typically be accompanied by surface rupture in regions where the seismogenic crustal thickness is on the order of 15 to 20 km and thus repeated events of this size will produce recognizable fault-related geomorphic features at the earth’s surface. However, the higher magnitudes used in this PSHA reflect (1) that crustal faults have received little attention in Chile and there are probably active faults in the site region that we have not accounted for, and (2) the seismogenic crust is thicker than 20 km

in the site region (27 ± 2 km). In this sense, the use of the term "background" is not accurate but we include these unknown seismic sources as part of the background seismicity.

In order to estimate probabilistic ground motions for the site, recurrence parameters are required for the background seismicity occurring within South American crust as well as for the intraslab earthquakes within the subducting Nazca plate. The recurrence relationships were estimated following the maximum likelihood procedure developed by Weichert [13] and estimated completeness intervals for the region. The relationships are in the form of the truncated exponential distribution for the occurrence of independent earthquakes. Dependent events, foreshocks, aftershocks, or smaller events within an earthquake swarm (the largest event is assumed to be a mainshock), were identified using empirical criteria for the size in time and space of foreshock-mainshock-aftershock sequences from the procedure adopted from Youngs *et al.* [14]. The resulting catalog for independent events was then used to develop the recurrence relationships.

The number of earthquakes were normalized on an annual basis and per unit area (km^2). The resulting recurrence relationship for crustal background earthquakes, assuming the usual form of the Gutenberg-Richter relationship of $\log N = a - bM$. For the crustal recurrence, 47 independent earthquakes (**M** 4.0 to 6.0) were used to establish a *b*-value of 1.04 for the crust. The crustal earthquake recurrence is not well constrained due to the small sample size and limited magnitude range. Predicted recurrence intervals for **M** 6.0 and **M** 7.0 and greater in the study region are 60 and 660 years, respectively.

In addition to the traditional approach of using areal source zones with uniformly distributed seismicity, Gaussian smoothing with a spatial window of 15 km was used to address the hazard from background seismicity and incorporate a degree of stationarity. The cell size used to calculate the hazard was 0.2 degrees. Minimum magnitude was **M** 3.0.

5.3 Megathrust

Several investigators, e.g., Nishenko [15] have recognized that the Peru-Chile subduction zone is segmented based on the historical record. For this study, we have adopted a model of the Peru-Chile subduction zone that consists of two segments (Fig.4). The model is based generally on the models of Contreras-Reyes and Carrizo [16] and Carena [17] although the boundaries between the two segments vary somewhat depending on the model. The model is derived from the historical seismicity along the subduction zone. The seismic source parameters and their weights for the megathrust segments are shown on Fig. 5.

The study region is located near the Mocha fault zone, which is the boundary between two segments: the Southern Chile segment, which ruptured in 1960 (between latitudes 48.0° ± 1.0°S. and 38.0° ± 1.0°S.) and the Concepción-Valparaiso segment, which is bounded on the north by the Challenger fault zone and Juan Fernandez Ridge (38.0° ± 1.0° S. to 31.0° ± 1.0° S.). We have included a 1.0° uncertainty in the segment boundaries because of (1) the uncertainty in defining the ends of the historical ruptures, (2) the boundaries may be broad zones, and (3) to allow partial ruptures onto adjacent segments, e.g., 2010 Maule earthquake.

The southern end of the Southern Chile segment coincides with the intersection of the Chile Rise with South America. The northern boundary of the segment appears to be well defined by ruptures in 1575, 1737, 1837, and 1960. Also note the disagreement for the 1837 earthquake. Carena [17] indicates the 1837 earthquake was a partial rupture with a magnitude of **M** 8 to 8.5. Contreras-Reyes and Carrizo [16] show a nearly full rupture of the Southern Chile segment.

The Concepción-Valparaiso segment appears to contain a range of partial ruptures from the 1657 (**M** 8.0) event to the 2010 **M** 8.8 Maule earthquake. In addition to a segmented Peru-Chile subduction zone, we include a small weight of 0.1 that it is unsegmented and allow an earthquake to float up and down the two segments with equal probability (Fig.5).

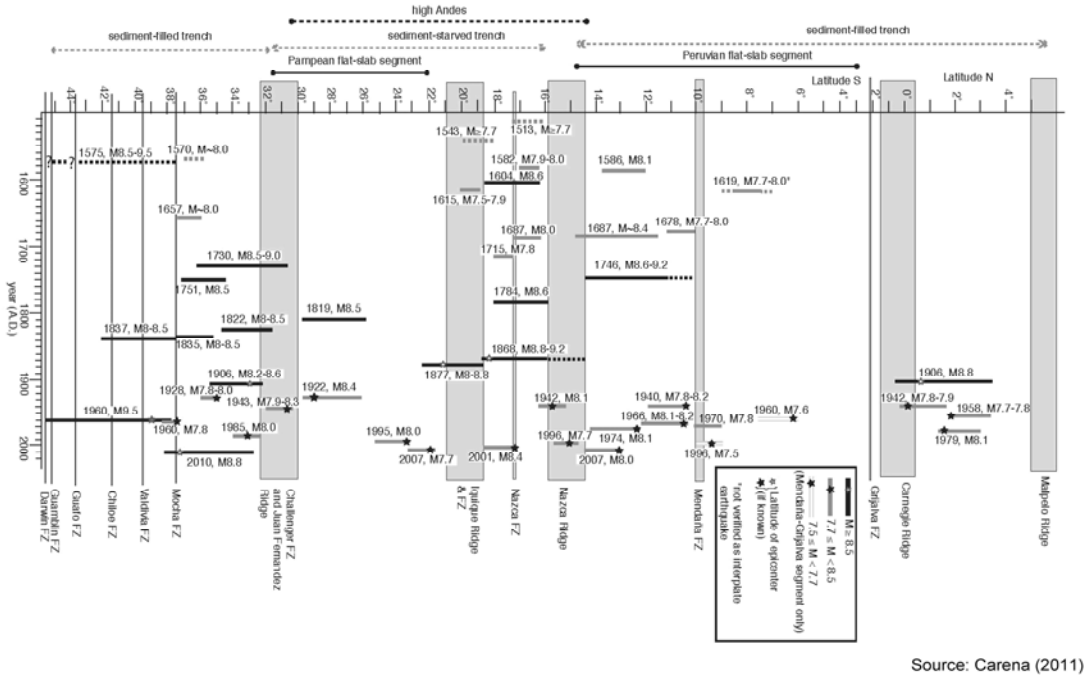

Fig. 4 – Space-time distribution of great earthquakes along Peru-Chile subduction zone.

In terms of recurrence models, for the Concepción-Valparaiso segment, we adopt the truncated exponential model with a weight of 1.0 because the historical ruptures along this segment cover the range of **M** 8.0 up to nearly **M** 9 (Fig.5). For the southern Chile segment, which may produce predominantly full ruptures, weights of 0.6, 0.3, and 0.1 were assigned to the maximum magnitude, characteristic, and truncated exponential models, respectively (Fig.5). These weights result in a total of 0.4 given to the possibility of smaller partial ruptures.

We assume that the maximum earthquakes have occurred already in historical times on the segments of the megathrust and have thus adopted the estimated maximum magnitudes observed to date with their uncertainties for the site region. For the Southern Chile segment that would be **M** 9.5 ± 0.1 and the Concepción-Valparaiso segment **M** 9.0 ± 0.2. For the unsegmented model, we adopt a **M** 9.0 ± 0.2.

The plate dips and maximum depths of the seismogenic megathrust along this portion of the subduction zone are generally similar. Modeling of the 2010 Maule earthquake indicates a dip of about 18° (USGS NEIC website) and 17° to 20° [7]. In earlier modeling of the 1928 **M** 7.8 and 1943 **M** 7.9 earthquakes in central Chile, Beck *et al*. [18] estimated dips of 20 to 30°. Based principally on the 2010 earthquake dip, we adopt a dip of 18° ± 2° for both segments. The top of the megathrust is placed at a depth of 5 km beneath the deformation front.

The maximum depth of the megathrust is not well constrained but it too is based on observations. The maximum depth of the 2010 Maule aftershocks was 45 to 50 km. The slip model of the 2010 event yielded a maximum depth of 45 km [7]. Beck *et al*. [18] obtained maximum depths of the 1922 and 1943 earthquakes of 40 km. We adopt a range of 45 ± 5 km for the PSHA.

To estimate recurrence along this portion of the Peru-Chile subduction zone, we have relied on the historical record. All the events in the Southern Chile segment have rupture lengths of 700 to 1000 km [15]. The mean recurrence between the 1575, 1737, 1837, and 1960 earthquakes is 128 ± 16 years [15]. However, we need the recurrence interval between characteristic events. None of the pre-1960 earthquakes appears to be a full rupture like the 1960 event although the uncertainties in defining the rupture lengths of these older events are large. Lomnitz [19] estimates a **M** 8 to 8.5 for the 1575 event which appears to be the largest of the three pre-1960 earthquakes. If the 1575 event is the predecessor of 1960, the interval between the two events is 385 years. Lomnitz [19] noted that large landslides blocked the outlet of Lake Rinihue as in 1960. Barrientos and Ward

[20] suggest that the recurrence intervals of **M** 9 + earthquake in Chile may be more than 300 years. Lomnitz [19] proposes that moment release in Chile may not be constant and discusses the possibility of clustering. Non-constant moment release would result in irregular recurrence intervals.

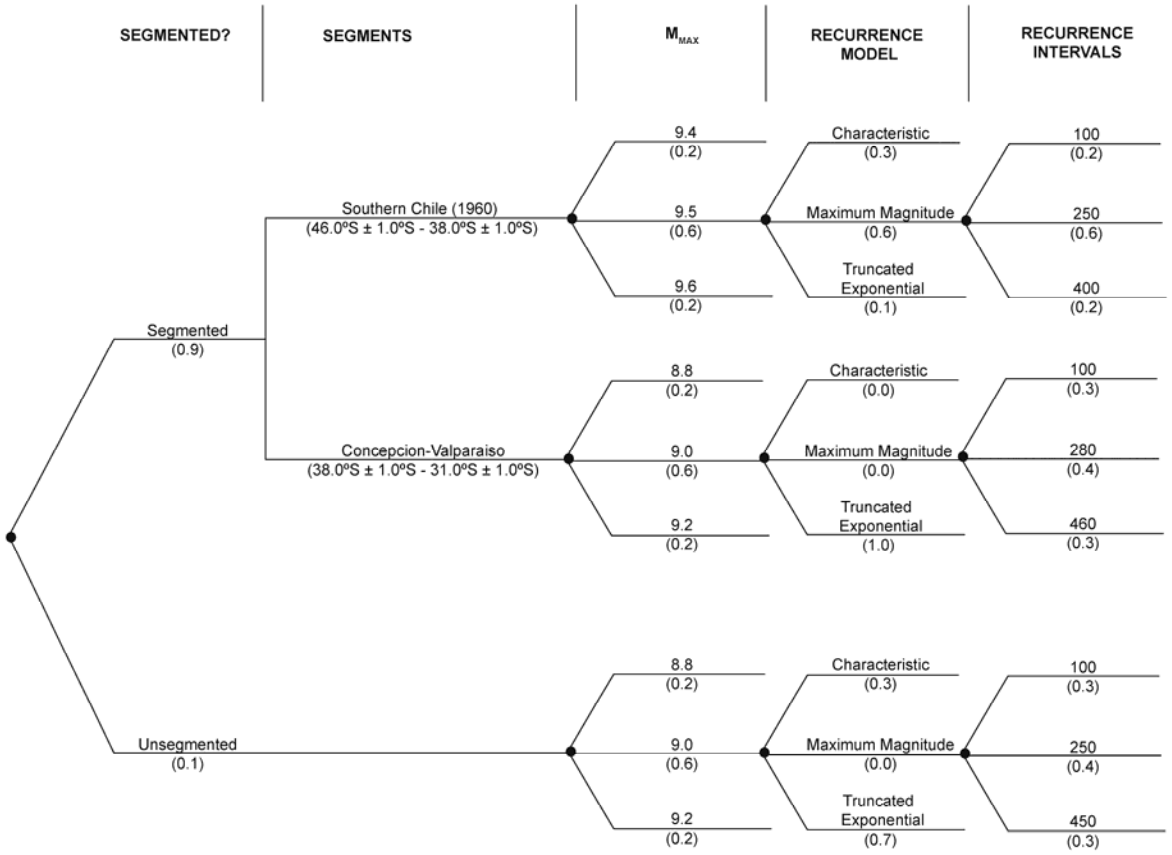

Fig. 5 – Peru-Chile subduction zone logic tree.

In the most comprehensive study of the 1960 earthquake, paleoseismic studies of buried soils and sand layers as records of tectonic subsidence and tsunami inundation at an estuary midway along the 1960 earthquake indicate that (1) the 1575 earthquake may have been the predecessor of 1960 and (2) the average recurrence of the past six 1960-type earthquakes in the past 2,000 years was about 300 years [21]. Based on the above, we adopt a range of recurrence intervals for the Southern Chile segment of 250 ± 150 years weighted 0.2, 0.6, and 0.2, respectively (Fig.5). This range would encompass the range of values discussed above.

For the Concepción–Valparaiso segment we adopt recurrence intervals of 280 ± 180 years (Fig.5). Here we assume that the 2010 event is characteristic of the segment event though it may not have fully ruptured the section from the Mocha fault zone to the Challenger fault zone. The only earthquake in this segment that is similar to 2010 in terms of size is the 1730 earthquake with an estimated **M** 8.5 to 9.0 [19]. The interval between these two earthquakes is 280 years. Because this is only a single recurrence interval, we include a large uncertainty of 180 years and use a wide distribution weighted 0.3, 0.4, and 0.3 (Fig.5).

Time-dependent or equivalent Poisson recurrence intervals were calculated for the Southern Chile and Concepcian-Valparaiso segments of the subduction megathrust. A lognormal renewal model, which is similar to the Brownian Passage (BPT) model, was used to compute the time dependent rates. A range of coefficient of variation (COV) of 0.3, 0.5 and 0.7 were used with weights of 0.2, 0.6, and 0.2, respectively. The COV is a measure of how peiodically earthquakes occur with a larger COV representing more random behavior. The distribution of COV was based on previous analyses by the authors. The time-dependent conditional probabilities of an event were converted to equivalent Poisson rates for hazard analyses using a 50-year time interval.

For the floating earthquake in the unsegmented model, we adopt recurrence intervals of 250 ± 150 years with a wide distribution (Fig.5). This recurrence interval distribution is simply an average distribution based on the estimates provided above for the two segments.

5.4 Wadati-Benioff zone

The largest known intraslab earthquake in the site region was the 1939 **M** 7.9 Chillán earthquake (Fig.2). Based on this event, the intraslab earthquakes are assumed to have a maximum magnitude of **M** 8.0 ± 0.2 beneath the study region. The Wadati-Benioff zone is modeled as a series of staircasing blocks of varying width depending on the along-strike length of the zone and 15 km thick to approximate the dipping Nazca plate. Unlike our megathrust model, we adopt a single intraslab region for the Chile subduction zone.

Similar to the approach taken for the crustal background seismicity, the recurrence was estimated for the intraslab zone assuming the truncated exponential model. A total of 227 independent intraslab earthquakes of **M** 4.0 to 7.9 were used to calculate a *b*-value of 0.96 for the intraslab earthquake source. The intraslab recurrence curve is well constrained and predicts recurrence intervals for **M** 6.0 and greater and **M** 7.0 and greater in the site region of about 6 and 54 years, respectively. The *b*-value was varied by ± 0.1 in the PSHA as was done for the crustal background zone.

6. Ground motion prediction

In this evaluation, the recently developed Pacific Earthquake Engineering Research (PEER) Center Next General Attenuation (NGA) models for the crustal earthquakes in tectonically active regions by Abrahamson *et al.* [22], Chiou and Youngs [23], Campbell and Bozorgnia [24], and Boore *et al.* [25] were used in the PSHA. These models have been shown to be applicable to regions worldwide.

Arango *et al*. [26] evaluated a set of global and regional subduction ground motion models for their applicability to Peru-Chile and Central America. This evaluation utilized a recently compiled database of strong motion data from Peru and Chile. Based on their evaluation, the models of Abrahamson *et al.* [27], Zhao *et al.* [28], Youngs *et. al.* [29], and Atkinson and Boore [30] were weighted equally. A comparison of the 2010 Maule strong motion data with the three ground motion prediction models show they match the data quite well. For the intraslab model, the same models for the megathrust were also equally weighted. We used a V_S30 of 270 m/sec for a generic soil site. Only the Abrahamson *et al.* [27] uses V_S30.

7. Hazard results

The results of the PSHA of the site are presented in terms of ground motion as a function of annual exceedance probability. This probability is the reciprocal of the average return period. Fig.6 shows the mean hazard curve for PGA for the four cities. Other spectral accelerations were also computed. The hazard is similar for the four cities. The building code 2475-year return period (2% exceedance in 50 years) PGA in Concepcion is 1.09g.

In Fig.7, the hazard curve contributions by seismic sources are shown for PGA for the city of Concepcion. The hazard is controlled by the megathrust at all return periods up to 5,000 years. The Wadati-Beioff zone is also a significant contributor to the PGA hazard. This pattern also applies to the other three cities. Fig.8 shows the megathrust dominating the longer period ground motions e.g., 1.0 sec spectral acceleration.

In Fig.9, we show the sensitivity of the PGA hazard to the selection of subduction zone ground motion prediction models. The hazard is moderately sensitive to the srlrvtion of both the megathrust and intraslab models.

In Fig.10, we computed the hazard using only the time-independent recurrence intervals and compare the hazard against the time-dependent hazard. The latter is lower because of the recent occurence of both the 1960 and 2010 earthquakes. At return periods of 475 and 2475 years, the time-dependent hazard is 21% and 18%

lower, respectively, than the time-independent hazard. This illistrates how important it is to evaluate time-dependent hazard in situations where the data are available. Such information can and should be used as part of risk-informed decision-making for hazard mitigation.

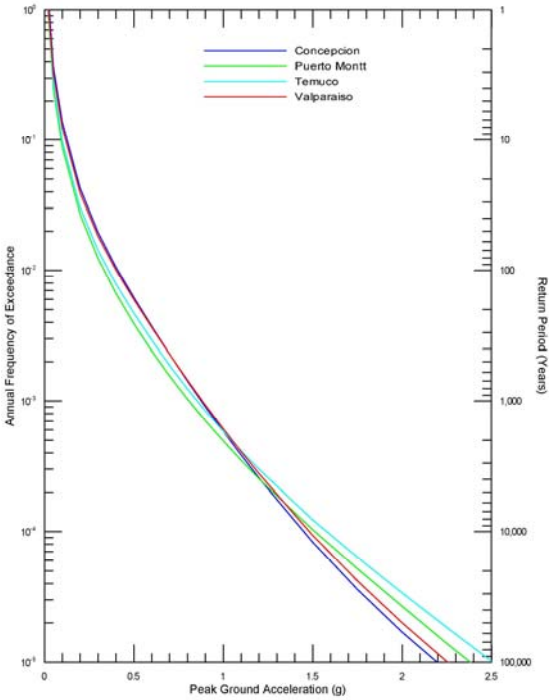

Fig. 6 – PGA hazard curves for four cities.

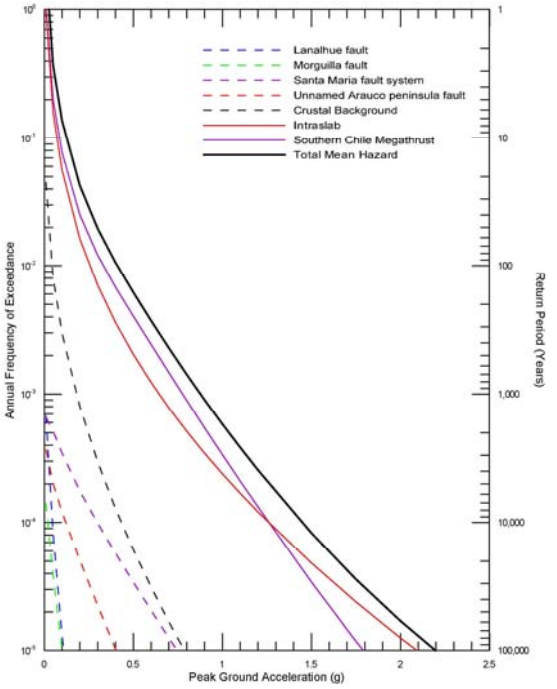

Fig. 7 – Seismic source contributions to horizontal PGA hazard in Concepcion.

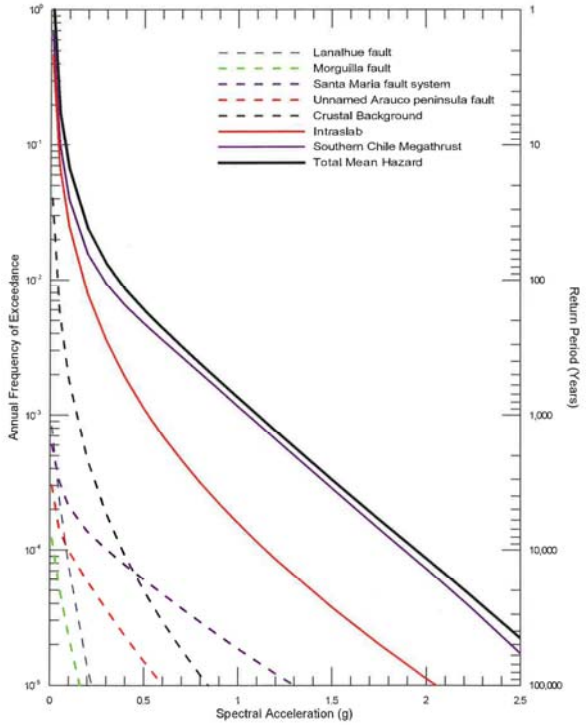

Fig. 8 – Seismic source contributions to horizontal 1.0 sec spectral acceleration in Concepcion.

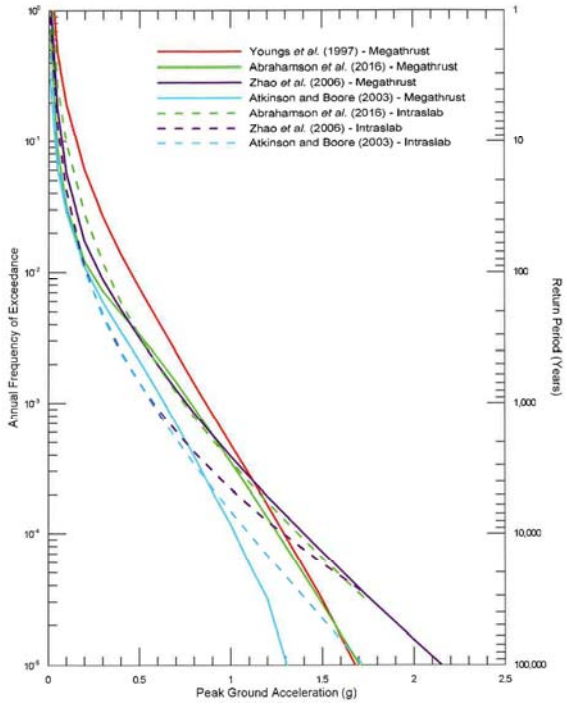

Fig. 9 – Sensitivity to selection of ground motion models to mean horizontal PGA hazard in Concepcion.

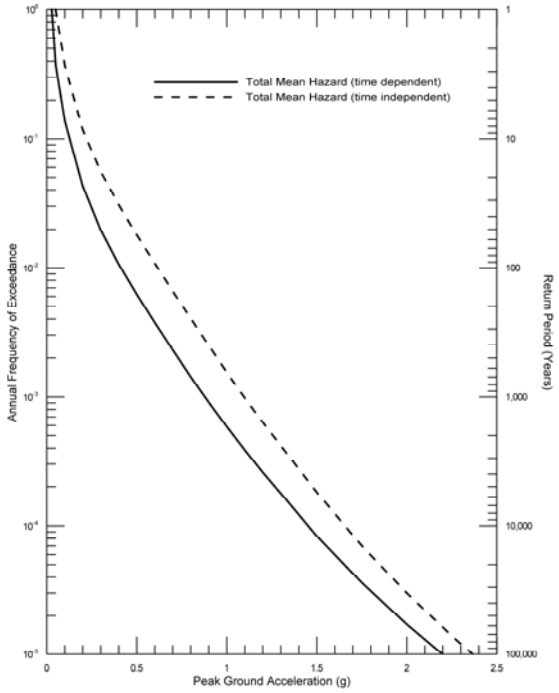

Fig. 10 – PGA hazard in Concepcion comparison of time-dependent and time-independent.

8. Acknowledgements

Our thanks to Julia Phillips, Ann Marie Holm, and Melinda Lee for their assistance in the preparation of this paper.

9. References

[1] Cornell CA (1968): Engineering seismic risk analysis. *Bulletin of the Seismological Society of America*, **58**(5), 1583-1606.

[2] Thomas PA, Wong IG, and Abrahamson NA (2010): Verification of probabilistic seismic hazard analysis software programs: *Report 2010/106*, Pacific Earthquake Engineering Research Center, Berkeley, USA.

[3] Rosenau M, Melnick D, and Echtler H (2006): Kinematic constraints on intra-arc shear and strain partitioning in the southern Andes between 38°S and 42°S latitude. *Tectonics*, **25**(4), TC4013.

[4] Wang K, Hu Y, Bevis M, Kendrick E, Smalley R Jr, Vargas RB, and Lauría E (2007): Crustal motion in the zone of the 1960 Chile earthquake: Detangling earthquake-cycle deformation and forearc-sliver translation. *Geochemistry, Geophysics, Geosystems*, **8**(10), Q10010.

[5] Moreno M, Klotz J, Melnick D, Echtler HP, and Bataille K (2008): Contemporary forearc deformation in south-central Chile from GPS observations (36-39° S)., *7th International Symposium on Andean Geodynamics (ISAG 2008, Nice)*, Extended Abstracts: 348-350.

[6] Melnick D, Bookhagen B, Strecker MR, and Echtler HP (2009): Segmentation of megathrust rupture zones from fore-arc deformation patterns over hundreds to millions of years, Arauco peninsula, Chile. *Journal of Geophysical Research*, **114**(B1), B01407.

[7] Vigny C, Socquet A, Peyrat S, Ruegg J-C, Metois M, Madariaga R, Morvan S, Lancieri M, Lacassin R, Campos J, Carrizo D, Bejar-Pizarro M, Barrientos S, Armijo R, Aranda C, Valderas-Bermejo M-C, Ortega I, Bondoux F, Baize S, Lyon-Caen H, Pavez A, Vilotte JP, Bevis M, Brooks B, Smalley R, Parra H, Baez J-C, Blanco M, Cimbara S, and Kendrick E (2011): The 2010 Mw 8.8 Maule megathrust earthquake of central Chile, monitored by GPS. *Science*, **332**(6036), 1417-1421.

[8] Melnick D, Moreno M, Motagh M, Cisternas M, and Wesson RL (2012): Splay fault slip during the Mw 8.8 2010 Maule Chile earthquake: *Geology*, published online on 23 January 2012 as doi:10.1130/G32712.1

[9] Haberland C, Riedbrock A, Lange D, Bataille K, Dahm T (2009): Structure of the seismogenic zone of the southcentral Chilean margin revealed by local earthquake traveltime tomography. *Journal of Geophysical Research*, **114**(B1), B01317.

[10] Lavenu A, Thiele R, Machette MN, Dart RL, Bradley L-A, and Haller KM (2000): Maps and Database of Quaternary Faults in Bolivia and Chile. U.S. Geological Survey Open-File Report 00-283.

[11] Wells DL and Coppersmith KJ (1994): New empirical relationships among magnitude, rupture length, rupture width, rupture area, and surface displacement. *Bulletin of the Seismological Society of America*, **84**(4), 974-1002.

[12] Hanks TC and Bakun WH (2008): M-logA observations for recent large earthquakes. *Bulletin of the Seismological Society of America*, **98**(1), 490-494.

[13] Weichert DH (1980): Estimation of the earthquake recurrence parameters for unequal observation periods for different magnitudes. *Bulletin of the Seismological Society of America*, **70**(4), 1337-1346.

[14] Youngs RR, Swan FH, Power MS, Schwartz DP, and Green RK (2000): Probabilistic analysis of earthquake ground shaking hazard along the Wasatch Front, Utah, *in* P.L. Gori and W.W. Hays (eds.), Assessment of Regional Earthquake Hazards and Risk Along the Wasatch Front, Utah. *U.S. Geological Survey Professional Paper 1500-K-R*, p. M1-M74.

[15] Nishenko SP (1991): Circum-Pacific seismic potential 1989-1999. *Pure and Applied Geophysics*, **135**(2), 169-259.

[16] Contreras-Reyes E and Carrizo D (2011): Control of high oceanic features and subduction channel on earthquake ruptures along the Chile-Peru subduction zone. *Physics of the Earth and Planetary Interiors*, **186**(1-2), 49-58.

[17] Carena S (2011): Subducting-plate topography and nucleation of great and giant earthquakes along the South American Trench. *Seismological Research Letters*, **82**(5), 629-637.

[18] Beck S, Barrientos S, Kausel E, and Reyes M (1998): Source characteristics of historic earthquakes along the central Chile subduction zone. *Journal of South American Earth Sciences*, **11**(2), 115-129.

[19] Lomnitz C (2004): Major earthquakes of Chile: a historical survey, 1535-1960. *Seismological Research Letters*, **75**(3), 368-378.

[20] Barrientos SE and Ward SM (1990): The 1960 Chile earthquake: inversion for slip distribution from surface deformation. *Geophysical Journal International*, **103**(3), 589-598.

[21] Cisternas M, Atwater BF, Torrejón F, Sawai Y, Machuca G, Lagos M, Eipert A, Youlton C, Salgado I, Kamataki T, Shishikura M, Rajendran CP, Malik JK, Rizal Y, and Husni M (2005): Predecessors of the giant 1960 Chile earthquake. *Nature*, **437**(7057), 404-407.

[22] Abrahamson NA, Silva WJ and Kamai R (2014): Summary of the ASK14 ground-motion relation for active crustal regions. *Earthquake Spectra*, **30**(3), 1025-1055.

[23] Chiou BSJ and Youngs RR (2014): Update of the Chiou and Youngs NGA ground motion model for average horizontal component of peak ground motion and response spectra. *Earthquake Spectra*, **30**(3), 1117-1153.

[24] Campbell KW and Bozorgnia Y (2014): NGA-West2 ground motion model for the average horizontal components of PGA, PGV, and 5%-damped linear acceleration response spectra. *Earthquake Spectra*, **30**(3), 1087-1115.

[25] Boore DM *et al.* (2014): NGA-West2 equations for predicting PGA, PGV, and 5% damped PSA for shallow crustal earthquakes. *Earthquake Spectra*, **30**(3), 1057-1085.

[26] Arango MC, Strasser FO, Bommer JJ, Cepeda JM, Boroschek R, Hernandez DA, and Tavera H (2012): An evaluation of the applicability of current ground-motion models to the South and Central American subduction zones. *Bulletin of the Seismological Society of America*, **102**(1), 143-168.

[27] Abrahamson NA, Gregor N, and Addo K (2016): BCHydro ground motion prediction equations for subduction earthquakes. *Earthquake Spectra*, **32**(1), 23-44.

[28] Zhao JX, Zhang J, Asano A, Ohno Y, Oouchi T, Takahashi T, Ogawa H, Irikura K, Thio HK, Somerville PG, Fukushima Y, and Fukushima Y (2006): Attenuation relations of strong ground motion in Japan using site classification based on predominant period. *Bulletin of the Seismological Society of America*, **96**(3), 898-913.

[29] Youngs RR, Chiou SJ, Silva WJ, and Humphrey JR (1997): Strong ground motion attenuation relationships for subduction zone earthquakes. *Seismological Research Letters*, **68**(1), 58-73.

[30] Atkinson GM, and Boore DM (2003): Empirical ground-motion relations for subduction zone earthquakes and their applications to Cascadia and other regions. *Bulletin of the Seismological Society of America*, **93**(4), 1703-1729.